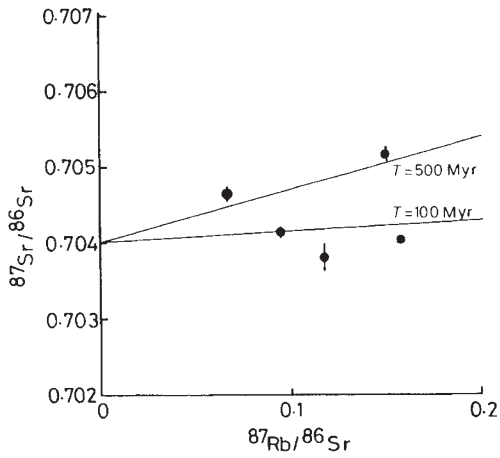

Fig. 4 $^{87}Sr/^{86}Sr$–$^{87}Rb/^{86}Sr$ diagram for the five pieces of Zaire cubic diamond. Lines in the figures are isochrons for 100 and 500 Myr, assuming initial values of 0.704 (refs 1 and 11).

all the elements under consideration in the cubic diamonds are recovered in the combustion method.

We have measured, for the first time, isotope ratios of Sr in the cubic diamonds (Table 2). As shown in Fig. 4, the isotope ratios of the five diamonds ranged from 0.7038 to 0.7052 and the variation of the isotope ratio does not show any correlation with Rb/Sr values. We can infer that the ages of the cubic diamonds are younger than several hundred Myr (the slopes of the lines in Fig. 4 correspond to isochrons of 100 and 500 Myr) and that the diamonds formed in rather heterogeneous environments or originated from different kimberlite pipes. Alternatively, Fig. 4 might indicate the effect of high-grade metamorphism. The result also indicates that the age of the diamonds, 6.0 Gyr, obtained by an isochron-like relation in the K–Ar system, is false.

Demaiffe and Fieremans[1] reported that Sr isotope ratios of Mbuji Mayi kimberlite and Kundelunge kimberlite of age 71 Myr (eruption age of the kimberlite) are 0.7038–0.7046, being different from those of diopside xenoliths in kimberlite (0.7031 + 0.0002). Their data do not form an isochron, which indicates that the kimberlites are heterogeneous in terms of the Rb–Sr system. Barrett and Berg reported a Sr isotope ratio of ~0.704 for fresh kimberlite. Our 71-Myr Sr isotope data (see Table 2) are almost identical to the values both in kimberlite and in carbonate inclusions[1] in kimberlite.

Navon *et al.*[3] consider that the fluid inclusion is pristine mantle fluid, the formation of which preceded the kimberlitic event. This conclusion is based on the difference in chemical composition between kimberlite and the diamonds. Our Sr isotope data favour a relation with kimberlite rather than with the mantle.

Boyd *et al.*[9] showed that carbon isotope ratios of cubic diamonds have a similar $\delta^{13}C$ value to that of the coat of the octahedral diamonds, which is different from the $\delta^{13}C$ of the core. From these results, they concluded that the cubic diamonds and the coat of octahedral diamonds are formed in a different location to the core of octahedral diamonds, and that the cubic diamonds and the coat of the octahedral diamonds might have formed in the same environment, perhaps in kimberlite, which all diamonds encountered.

Our Sr isotope ratio and chemical studies of the cubic diamonds suggest that the cubic diamonds grew in the volatile-rich fluid in the kimberlite or the precursory kimberlite. The carbon isotope ratio of kimberlite shows a larger deviation than that of cubic diamonds[10]. To explain both the excess ^{40}Ar and the small deviation in carbon isotope ratio of the cubic diamond, some way of collecting volatiles from a large volume of the kimberlite and of averaging the carbon isotope ratio must be found[7]. Kimberlite must have had a low viscosity before eruption and the volatiles could easily have moved in the kimberlite body. The difference in chemical compositions observed between kimberlite and the cubic diamonds (this study and ref. 3) may be mainly a result of chemical partitionings of elements between the kimberlite and the volatile-rich fluid, as incompatible elements are incorporated preferentially into the fluid.

Received 22 August; accepted 31 October 1988.

1. Demaiffe, D. & Fieremans, M. *Chem. Geol.* **31**, 311–323 (1981).
2. Melton, C. E. & Giardini, A. A. *Am. Miner.* **59**, 775–782 (1974).
3. Navon, O., Hutcheon, I. D., Rossman, G. R. & Wasserburg, G. J. *Nature* **335**, 784–789 (1988).
4. Zashu, S., Ozima, M. & Nitoh, O. *Nature* **323**, 710–712 (1986).
5. Akagi, T. & Masuda, A. *Geochem. J.* **22**, 81–82 (1988).
6. Podosek, F. A., Pier, J., Nitoh, O., Zashu, S. & Ozima, M. *Nature* **334**, 607–609 (1988).
7. Masuda, A. & Akagi, T. *Geochem. J.* **22**, 139–142 (1988).
8. Kramers, J. D., Smith, C. B., Lock, N. P., Harmon, R. S. & Boyd, F. R. *Nature* **291**, 53–56 (1981).
9. Boyd, S. R. *et al. Earth planet. Sci. Lett.* **86**, 341–353 (1987).
10. Javoy, M., Pineau, F. & Demaiffe, D. *Earth planet. Sci. Lett.* **68**, 399–412 (1984).
11. Barrett, D. R. & Berg, G. W. *Phys. Chem. Earth* **9**, 619–635 (1975).
12. Masuda, A., Nakamura, N. & Tanaka, T. *Geochim. cosmochim. Acta* **37**, 239–248 (1973).
13. Gopalan, K. & Wetherill, G. W. in *Handbook of Elemental Abundances in Meteorites* (ed. Mason, B.) 297–302 (Gordon and Breach, New York, 1971).
14. Goles, G. G. in *Handbook of Elemental Abundances in Meteorites* (ed. Mason, B.) 285–296 (Gordon and Breach, New York, 1971).

The Dupal anomaly as a trace of the upwelling lower mantle

Pat Castillo*

Department of Terrestrial Magnetism, Carnegie Institution of Washington, 5241 Broad Branch Rd, NW, Washington, DC 20015, USA

It is now widely accepted that the Earth's mantle is isotopically heterogeneous, but the scale and distribution of this heterogeneity and the structure and evolution of the mantle as a whole are poorly understood. The 'Dupal anomaly'[1,2] has an important bearing on this problem because it is the largest isotopic domain yet delineated on the Earth's surface and it is suggested[2] to have been formed early in the Earth's history. Here I show that the two Dupal anomaly maxima appear to be closely associated with the two large-scale regions of low seismic velocity in the lower mantle[3], which in turn are correlated with the loci of active hotspots. This correlation raises the possibility that large-scale structural features in the lower mantle produce geochemical imprints on the Earth's surface. Thus, the correlation may place severe constraints on the chemical structure of the mantle and the nature of mantle convection.

Dupré and Allègre[1] recognized that lavas from oceanic islands in the South Atlantic and Indian Ocean have high $^{87}Sr/^{86}Sr$ ratios (>0.7035) and anomalously high $^{207}Pb/^{204}Pb$ and $^{208}Pb/^{204}Pb$ ratios for a given $^{206}Pb/^{204}Pb$ ratio compared with North Atlantic and East Pacific islands. Hart[2] termed this isotope signature and its geographical distribution on the ocean floor the 'Dupal anomaly' and showed that although the strongest maximum of the anomaly stretches from the Indian Ocean to the South Atlantic Ocean, a second maximum with an only slightly high $^{207}Pb/^{204}Pb$ ratio exists in the southern Central Pacific Ocean. Hart[2] also suggested that the two maxima are connected, forming a globe-encircling belt centred on latitude 30° S. The two Dupal anomaly maxima appear to be located above the minima of the two large-scale regions of low seismic velocity (LVRs) in the lower mantle[3], as well as above concentrations of the majority of active hotspots[4] (Fig. 1).

The LVRs in the lower mantle are beneath the southern Central Pacific and the southern tip of Africa, with the latter extending beneath the Eastern Atlantic Ocean (negative contours in Fig. 1). The LVRs are surrounded by high-seismic-

* Present address: Division of Marine Geology and Geophysics, Rosenstiel School of Marine and Atmospheric Science, University of Miami, Miami, Florida 33149, USA.

© 1988 Nature Publishing Group

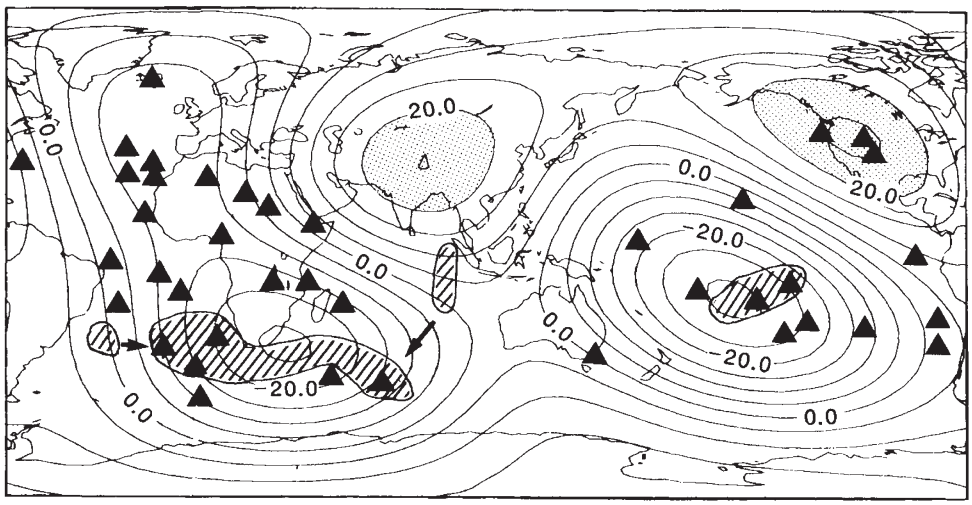

Fig. 1 World map showing model L02.56 of the three-dimensional P-wave velocity distribution averaged for the whole lower mantle using orders two and three[3,8] (contoured in m s^{-1}), the locations of hotspots[4,8] (triangles), and the Dupal anomaly maxima in the Indian–South Atlantic and Central Pacific regions[1,2] (hatched areas). Dupal maxima for the Ninety-east Ridge (central hatched area) and Rio Grande Rise (far left hatched area) are samples of old hotspot traces and should be plotted at the locations of their origin (indicated by arrows). Velocity regions higher than 20 m s^{-1} are shown stippled. Note that the Dupal anomaly maxima and the LVR minima are correlated; the majority of hotspots are above the LVRs.

velocity regions (HVRs) which are well correlated with the locations of present and geologically recent subduction zones. The good correlation between the tomographically observed HVRs and subduction zones, and more direct observations of seismically fast extensions of subduction zones deep into the lower mantle, have led some investigators[5–8] to believe that subducted slabs continue to sink into the lower mantle, perhaps all the way to core–mantle boundary. The subducted slabs that penetrate the lower mantle must, however, be accompanied by an equal mass returning back to the upper mantle in order to conserve mass. Accordingly, Silver *et al.*[8] suggested that LVRs represent complementary return flows of the subducted materials and that large hotspot volcanism (such as that found in Hawaii and Gough) is a manifestation of these return flows. Thus, the apparent correlation between the locations of the Dupal anomaly maxima, LVRs and hotspot concentrations suggests that the Dupal isotope signature may simply originate from hotter, upwelling regions of the lower mantle and/or the LVRs are causing at least the upper mantle, or perhaps portions of lithosphere, to produce the Dupal isotope signature. In other words, the Dupal anomaly could potentially provide a strong constraint on mantle convection, if a direct correlation between the features of the lower mantle and the geochemical properties of the Earth's surface can be established.

As a first step in establishing the correlation, it has to be shown that the two Dupal anomaly maxima, like the LVRs and hotspot concentrations, are not connected. The Dupal anomaly maxima have been delineated[2] by using Sr and Pb isotope data of mostly ocean island basalts (OIBs) and a few continental and subduction zone basalts. Most ocean islands, however, are built by hotspots that are generally confined within the LVRs, and data of more regional extent are therefore needed to better trace the geographical extent of the Dupal anomaly. Mid-ocean-ridge basalts (MORBs) can provide this extra needed information because unlike OIBs, which are erupted in clusters of volcanic centres, MORBs are erupted along an interconnecting, worldwide network of volcanoes. MORBs are more voluminous than OIBs and these lavas represent continuous samples of large regions of the mantle, including those regions that fill the gaps between the two Dupal anomaly maxima (that is, regions of the mantle under the East Pacific Rise (EPR) at 30° S and the Southeast Indian Ridge (SEIR)).

Figure 2 shows the ΔSr, Δ7/4 and Δ8/4 values of published and unpublished MORB Sr and Pb isotope data calculated according to the procedure of Hart[2], wherein this Δ representation is defined. North Atlantic and Pacific MORB ΔSr, Δ7/4 and Δ8/4 background values are typically ~25, 0 and 0, respectively but MORB ΔSr values that are >25, with corresponding positive Δ7/4 and Δ8/4 values (which constitutes the Dupal isotope signature), are present at intervals along the entire ridges. Bearing in mind the lack of data in many areas along the ridges, the Dupal anomaly appears to be strong at (1) the whole Carlsberg–Central Indian Ridge (CIR), (2) the Southwest Indian Ridge (SWIR) to ~50° S latitude, (3) the south Mid-Atlantic Ridge (MAR) from ~25° S to ~55° S latitude, and (4) the SEIR as far as ~124° E longitude[10]. As shown previously[11,12], there is no consistent and strong Dupal anomaly anywhere along the EPR. Based mainly on ΔSr and a few highly variable Δ8/4 values, there appears to be a small Dupal anomaly in Atlantic MORBs near the Azores where the extension of the African LVR is located. More Pb isotope data are needed for these lavas to confirm this point, but the work of Shirey *et al.*[13] on Oceanographer Fracture Zone lavas at 35° N latitude, and available Sr and Pb isotope data for the Azores lavas[2,14,15], show clear indications of the Dupal signature.

Thus the combined data from Figs 1 and 2 show the following. (1) There is a fairly good correlation between the locations of the Dupal anomaly maxima and LVR minima in the Southern Hemisphere; both the Dupal maxima and LVR minima are disconnected and are separated by HVRs in the lower mantle[3] under Australia and South America. (2) The majority of the hotspots are concentrated near LVRs; some hot spots near the LVR minima (for example, St Helena and Tubuaii), however, do not have the Dupal isotopic composition. (3) There appears to be a Dupal anomaly near the Azores, where a third but less pronounced LVR is located. (4) The magnitudes of the correlated phenomena are variable. The Dupal anomaly maximum associated with the most pronounced LVR in the Pacific generally does not have an anomalously high Δ7/4 value and it has a smaller areal extent; the anomaly maximum associated with the intermediate LVR in Africa has a larger areal extent. More recent Sr and Pb isotope data for islands and aseismic ridges near the LVR in the Pacific[16,17] apparently do not indicate significant changes in the general areal distribution and magnitude of the Pacific anomaly. The Dupal anomaly near the Azores, if present, is the weakest in terms of the Δ7/4 and Δ8/4 values. (5) MORBs with Dupal isotopic characteristics are present at places in all ridges.

Note that the difference in isotopic compositions between MORBs from the EPR on the one hand, and MORBs from the MAR and Indian ridges (that is, those bearing the Dupal isotope signature) on the other, has been suggested[18,19] to be due to the fast spreading rate of the EPR. Batiza[18] and Allègre *et al.*[19] argued that mixing of mantle components under the faster-spreading EPR is more efficient than under the slower-spreading MAR, and especially more so than under the Indian mid-ocean ridges. But Ito *et al.*[20] showed that this cannot be the only cause of the difference (this is also borne out in Fig. 2). ΔSr, Δ7/4

© 1988 Nature Publishing Group

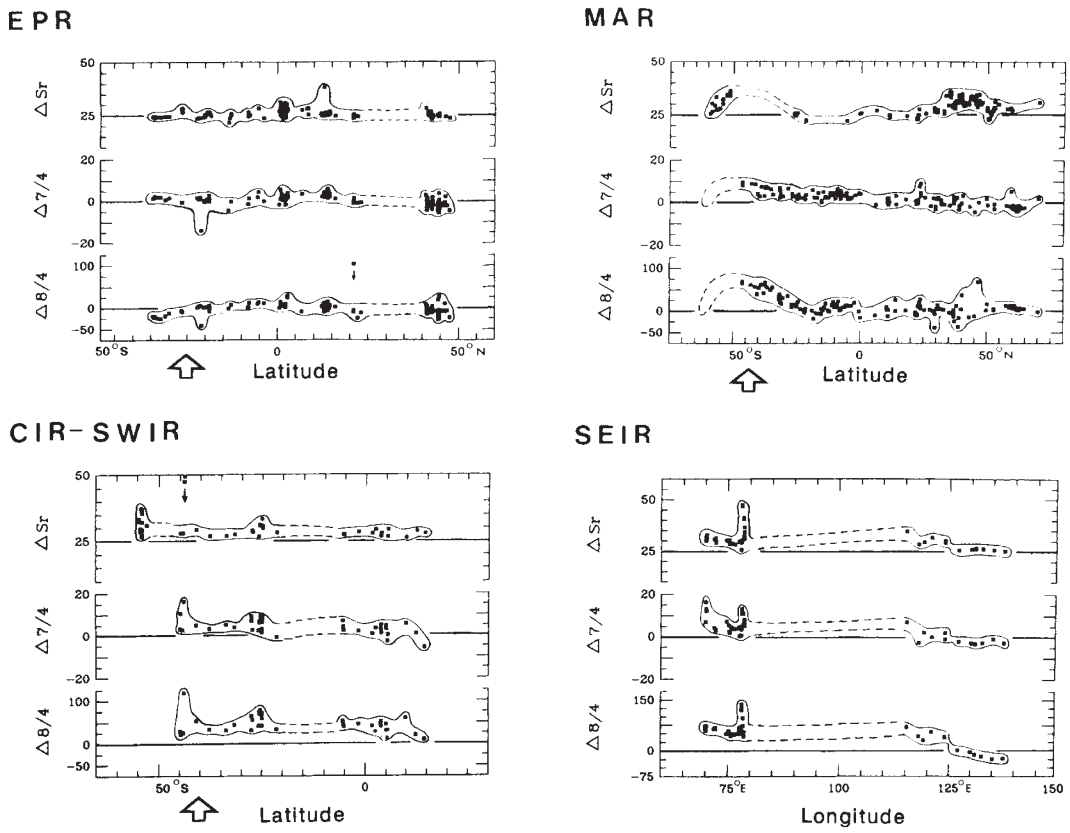

Fig. 2 ΔSr, Δ7/4 and Δ8/4 values for MORBs from the world's ridge systems plotted against locations. These values, represented by solid squares, are enclosed by solid curves (dashed curves in areas where there are no data), and background values are drawn as solid lines for clarity. A few data points (with small, solid arrows pointing downward) have unusually high values and are not enclosed within the solid curves. Errors of ΔSr, Δ8/4 and Δ7/4 values are dependent upon analytical precision of Sr and Pb isotopic ratios but are generally ~2%, 3% and 10% respectively. Open arrows below the EPR, MAR and CIR-SWIR diagrams point to approximate locations of the Dupal anomaly belt as suggested by Hart[2]; the SEIR segment plotted runs subparallel to this belt. There is a lack of data along some segments of the ridges, but on average, values are above background at about 25° to 55° S latitude in the MAR, in the CIR-SWIR except in the northernmost part, and in the SEIR except for those east of 124° E longitude. Values for ΔSr and a few for Δ8/4 at about 30° to 50° N latitude in the MAR are also above background. The projected high ΔSr values for the south MAR are based on preliminary results of Cole *et al*[9]. Although exhibiting some spikes, EPR values straddle the background values. Data are from Castillo, Shirey and the CHEPR team (unpublished data), Castillo and Batiza (unpublished data), and from the literature.

and Δ8/4 values between the northern and southern segments of the EPR do not differ very much, although the spreading rates of these segments vary by a factor of three. Conversely, spreading rates between the northern and southern segments of MAR do not differ significantly, although the ΔSr, Δ7/4 and Δ8/4 values of the southern segment are distinctly higher (corresponding to the Dupal signature) and more heterogeneous than those of the northern segment. The spreading rate of the SEIR east and west of the Australian-Antarctic Discordance (AAD) also does not change significantly, but the ΔSr, Δ7/4 and Δ8/4 values for MORBs west of this boundary are higher (Dupal-like) than those for MORBs to the east[10].

Schilling and co-workers[21,22] and Hamelin *et al.*[23] have suggested that the provinciality of MORB composition, particularly that of MORBs from the south MAR and Indian ridges, is due to mixing of hotspot plume(s) and the depleted component of the upper mantle. This mixing phenomenon is clearly demonstrated in MORBs near hotspots (such as Galapagos, Iceland and Bouvet). Plume influence is mostly localized, however, and is expected to decrease at a rate that is proportional to the square root of hotspot distance from the ridge[22]. As shown in Fig. 2, the Dupal isotope signature of MORBs covers large regions including areas well away from hotspots. For example, the 22°-31° S segment of the MAR is supposed to be free from hotspot influence based on the plume-mixing model[22], but lavas from young, isolated seamounts near this segment have the Dupal isotope signature[24]. In comparison, lavas from young, isolated seamounts near the EPR segments remote from hotspots do not have the Dupal signature[24]. (Lavas from young seamounts near mid-ocean ridges and MORBs come from the same upper-mantle source[18,24-26].) This point is also illustrated by the lavas from the SEIR segment west of the AAD, which have the Dupal isotope signature despite the fact that the segment is far (~4,000 km) from a Dupal hotspot in the Indian Ocean. Note that the Western Victoria hotspot is near (~1,500 km) this region of the SEIR and its lavas also have the Dupal signature[2]. The hotspot, however, is in the east-northeast side of the AAD, wherein SEIR lavas do not have the Dupal signature. Therefore, it appears that the Dupal isotope signature of MORBs reflects the regional isotopic composition of the underlying mantle rather than the influence of hotspots. Some hotspots, especially those in the Southern Hemisphere (for example, Tristan, Gough, Kerguelen and Samoa), indeed contribute to the Dupal signature of nearby MORBs, but as a whole, hotspots have variable sizes and life spans and most importantly, their lavas have different chemical and isotopic characteristics.

In summary, there is, to a first approximation, a good correlation among the locations of the OIB Dupal anomaly maxima, LVRs and hotspot concentrations. Complementary MORB Sr and Pb isotope data strengthen this correlation. Data indicate that the Dupal anomaly can be subdivided into two (or three) sub-domains: Pacific and Indian-South Atlantic (with a minor component beneath the Azores). The locations of these Dupal maxima are correlated with the Pacific and African (plus Azores) LVR, respectively, which suggests that the Dupal isotope signature is originating from the lower mantle. Previously suggested spreading-rate and plume origins of the Dupal isotope signature in MORBs from the Indian Ocean and south MAR appear to be inconsistent with all available data.

The above correlation between tomographic features in the lower mantle and the isotopic characteristics of the oceanic crust is based on presently available data. Obviously, these are global features, and therefore more data are needed to verify or nullify such a relationship. But if the correlation exists it will give rise to questions such as why the geophysical structure of the lower mantle is reflected in the geochemistry of erupted rocks, whether

© 1988 Nature Publishing Group

the Dupal anomaly is a tracer of motions in the lower mantle, whether the Dupal anomaly is a signature of the subcontinental mantle[13,29,30] or of lower-mantle compositions, and whether the LVRs are return flows of previously subducted slabs. A resolution of the correlation will undoubtedly lead to further important discoveries related to chemical geodynamics[27,28].

The author is very grateful to P. Silver, R. Carlson, S. Shirey and J. Morris for helpful discussions. Their reviews and those by D. Gerlach, R. Batiza, J. Bender, G. Davies and friends at DTM are also acknowledged.

Received 30 May; accepted 3 November 1988.

1. Dupré, B. & Allègre, C. J. *Nature* **303,** 142–146 (1983).
2. Hart, S. R. *Nature* **309,** 753–757 (1984).
3. Dziewonski, A. M. *J. geophys. Res.* **89,** 5929–5952 (1984).
4. Stefanik, M. & Jurdy, D. *J. geophys. Res.* **89,** 9919–9925 (1984).
5. Jordan, T. H. *J. Geophys.* **43,** 473–496 (1977).
6. Craeger, K. C. & Jordan, T. H. *J. geophys. Res.* **91,** 3573–3589 (1986).
7. Silver, P. G. & Chan, W. W. *J. geophys. Res.* **91,** 13787–13802 (1986).
8. Silver, P. G., Carlson, R. W. & Olson, P. *A. Rev. Earth planet. Sci.* **16,** 477–541 (1988).
9. Cole, M. W., Hanan, B. B., Kingsley, R. & Schilling, J.-G. *Eos* **66,** 408 (1985).
10. Klein, E. M., Langmuir, C. H., Zindler, A., Staudigel, H. & Hamelin, B. *Nature* **333,** 623–629 (1988).
11. Macdougal, J. D. & Lugmair, G. W. *Earth planet Sci. Lett.* **77,** 273–284 (1986).
12. White, W. M., Hofmann, A. W. & Purchelt, H. *J. geophys. Res.* **92,** 4881–4893 (1987).
13. Shirey, S. B., Bender, J. F. & Langmuir, C. H. *Nature* **325,** 217–223 (1987).
14. Hawkesworth, C. J., Norry, M. J., Roddick, J. C. & Vollmer, R. *Nature* **280,** 28–31 (1979).
15. Dupré, B., Hamelin, B., Allègre, C. J. & Manhes, G. *US Geol. Survey Open File Rep.* **103,** 78–701 (1978).
16. Dupuy, C., Vidal, P., Barszus, H. G. & Chauvel, C. *Earth planet. Sci. Lett.* **82,** 145–152 (1987).
17. Wright, E. & White, W. M. *Earth planet. Sci. Lett.* **81,** 151–162 (1986/1987).
18. Batiza, R. *Nature* **309,** 440–441 (1984).
19. Allègre, C. J., Hamelin, B. & Dupré, B. *Earth planet Sci. Lett.* **71,** 71–84 (1984).
20. Ito, E., White, W. M. & Gopel, C. *Chem. Geol.* **62,** 157–176 (1987).
21. Schilling, J.-H. *Earth planet Sci. Lett.* **25,** 103–115 (1975).
22. Hanan, B. B., Kingsley, R. H. & Schilling, J.-G. *Nature* **322,** 137–144 (1986).
23. Hamelin, B., Dupré, B. & Allègre, C. J. *Earth planet Sci. Lett.* **67,** 340–350 (1984).
24. Batiza, R. & Castillo, P. R. *Eos* **69,** 491 (1988).
25. Zindler, A., Staudigel, H. & Batiza, R. *Earth planet Sci. Lett.* **70,** 175–195 (1984).
26. Batiza, R. & Vanko, D. *J. geophys. Res.* **89,** 11235–11260 (1984).
27. Allègre, C. J. *Tectonophysics* **81,** 395–400 (1982).
28. Zindler, A. & Hart, S. R. *A. Rev. Earth planet. Sci.* **14,** 493–571 (1986).
29. Gerlach, D. G., Hart, S. R., Morales, V. W. & Palacios, C. *Nature* **322,** 165–169 (1986).
30. Hawkesworth, C. J., Mantovani, M. S. M., Taylor, P. N. & Palacs, Z. *Nature* **322,** 356–359 (1986).

Theoretical evidence for a new ultra-high-pressure phase of SiO_2

Key Taeck Park*, Kiyoyuki Terakura* & Yoshito Matsui†

* Institute for Solid State Physics, University of Tokyo, Roppongi, Minato-ku, Tokyo 106, Japan
† Institute for Study of the Earth's Interior, Okayama University, Misasa, Tottori-ken 682-02, Japan

A phase of silica denser than stishovite (SiO_2-rutile) has been searched for intensively. Following the suggestions by Al'tshuler *et al.*[1] and Simakov *et al.*[2], SiO_2-fluorite was once regarded as a candidate for such a high-pressure phase. Subsequent theoretical studies[3,4] revealed, however, that SiO_2-fluorite would have at most about the same density as SiO_2-rutile and that it would be dynamically unstable at pressures below 170 GPa (ref. 4). Here we propose an alternative hypothetical polymorph of silica with a modified fluorite ($Pa\bar{3}$) structure as a possible high-pressure phase. SiO_2-$Pa\bar{3}$ would have a density of 4.46 g cm^{-3} (~6% denser than SiO_2-rutile at normal pressures) and should become more stable than SiO_2-rutile at pressures of $\gtrsim$60 GPa. These results also suggest that $MgSiO_3$-perovskite, which is widely accepted as the major constituent within the Earth's deep interior, may be unstable at very high pressure.

The present arguments are based on first-principles electronic-structure calculations for SiO_2-fluorite, -rutile and -$Pa\bar{3}$, the crystal structures of which are shown in Fig. 1. SiO_2-$Pa\bar{3}$ was predicted theoretically as a stable phase in a molecular-dynamics study of SiO_2-fluorite[5]. However, its optimal structure and relative stability with respect to other phases could not be inferred unambiguously from this previous work because of the use of simplified classical interatomic potentials with uncertain ranges of applicability. We have attempted to obtain such information using first-principles electronic-structure calculations.

We used the local-density approximation (LDA) in density functional theory[6] and the full-potential linear augmented plane wave (FLAPW) method[7,8] to solve the resultant effective one-electron problem. To limit the number of plane-wave basis functions, we used an energy cutoff of 22 Rydbergs, which results in a maximum dimension of ~850 for the hamiltonian matrix of SiO_2-$Pa\bar{3}$. The numbers of k points in the first Brillouin zone for the k-space integration are 32, 8 (16) and 8 (32) for SiO_2-fluorite, -rutile and -$Pa\bar{3}$, respectively. (The numbers in the parentheses denote the numbers of k points equivalent to SiO_2-fluorite for equal numbers of atoms in a unit cell.) For insulators, these numbers are sufficient to obtain structural information. We found that the results for SiO_2-rutile were affected only marginally by doubling the number of k points used. The $3s$ and $3p$ states of Si and the $2s$ and $2p$ states of O were treated as valence states and we adopted a single energy window, which is sufficient when, as in this case, there is no problem of shallow semicores. The combination of the LDA and the pseudo-potential method has been applied successfully to several systems, including α-cristobalite[9]. As the FLAPW method is no less accurate than the pseudo-potential method, the present approach is expected to be fairly reliable for discussing the structure of silica. The reliability of our calculations may be judged by Table 1, where our results are compared with those of other theoretical studies and also with available experimental data.

Figure 2 shows the calculated total energies as a function of volume for SiO_2-fluorite, -rutile and -$Pa\bar{3}$. For SiO_2-fluorite, the crystal structure is uniquely determined by its volume, and the total-energy calculation for a given volume is straightforward. The present result, denoted by the long-dashed curve, agrees fairly well with those from other sources, as shown in Table 1. On the other hand, for SiO_2-rutile and -$Pa\bar{3}$, arbitrary parameters (c/a and u for rutile and u for $Pa\bar{3}$) arise in the optimization of the structure for a given volume. Here, a and c are unit-cell dimensions; for SiO_2-rutile, u is defined such that the nearest Si–O distance in the c-plane is given by $\sqrt{2}ua$, whereas in

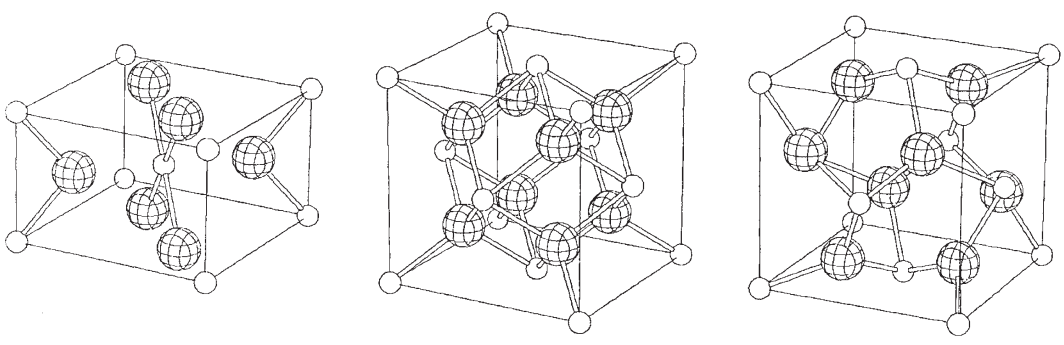

Fig. 1 From left to right, the unit cells of SiO_2 with rutile, fluorite and $Pa\bar{3}$ structures, respectively. Si is denoted by a small open sphere and O by a large hatched one. Nearest-neighbour atoms are connected by bars.

© 1988 Nature Publishing Group